NADH-Regulated Metabolic Model for Growth of *Methylosinus trichosporium* OB3b. Cometabolic Degradation of Trichloroethene and Optimization of Bioreactor System Performance

E. Marijn Sipkema,[†] Wim de Koning,[‡] Klaassien J. Ganzeveld,*[,†] Dick B. Janssen,[‡] and Antonie A. C. M. Beenackers[†]

Chemical Engineering and Biochemistry Departments, University of Groningen, NL-9747 AG Groningen, The Netherlands

A metabolic model describing growth of *Methylosinus trichosporium* OB3b and cometabolic contaminant conversion is used to optimize trichloroethene (TCE) conversion in a bioreactor system. Different process configurations are compared: a growing culture and a nongrowing culture to which TCE is added at both constant and pulsed levels. The growth part of the model, presented in the preceding article, gives a detailed description of the NADH regeneration required for continued TCE conversion. It is based on the metabolic pathways, includes Michaelis−Menten type enzyme kinetics, and uses NADH as an integrating and controlling factor. Here the model is extended to include TCE transformation, incorporating the kinetics of contaminant conversion, the related NADH consumption, toxic effects, and competitive inhibition between TCE and methane. The model realistically describes the experimentally observed negative effects of the TCE conversion products, both on soluble methane monooxygenase through the explicit incorporation of the activity of this enzyme and on cell viability through the distinction between dividing and nondividing cells. In growth-based systems, the toxicity of the TCE conversion products causes rapid cell death, which leads to wash-out of suspended cultures at low TCE loads (below μM inlet concentrations). Enzyme activity, which is less sensitive, is hardly affected by the toxicity of the TCE conversion products and ensures high conversions (>95%) up to the point of wash-out. Pulsed addition of TCE (0.014−0.048 mM) leads to a complete loss of viability. However, the remaining enzyme activity can still almost completely convert the subsequently added large TCE pulses (0.33−0.64 mM). This emphasizes the inefficient use of enzyme activity in growth-based systems. A comparison of growth-based and similar non-growth-based systems reveals that the highest TCE conversions per amount of cells grown can be obtained in the latter. Using small amounts of methane (negligible compared to the amount needed to grow the cells), NADH limitation in the second step of this two-step system can be eliminated. This results in complete utilization of enzyme activity and thus in a very effective treatment system.

Introduction

The presence of volatile chlorinated hydrocarbons such as trichloroethene (TCE), both in industrial waste streams and in contaminated surface and groundwater, asks for efficient remediation techniques. As a result of the mild conditions used and the often low costs of nutrients, biological breakdown constitutes a feasible alternative to conventional processes (*2*, *3*) such as active carbon adsorption and incineration (*4*). However, many chlorinated ethenes do not support growth and can, under aerobic conditions, only be converted by cometabolism. In this process, contaminant conversion results from the nonspecificity of one of the cellular oxygenating enzymes, and an additional primary substrate is needed for growth. Of the organisms that have been shown to convert TCE, the methanotroph *Methylosinus trichosporium* strain OB3b appears to have the best characteristics for application in remediation systems (*5*, *6*). These cells use a cheap and widely available growth substrate and express under copper limitation soluble methane monooxygenase (sMMO) (*7*−*10*), an enzyme with high specific activities for almost all chlorinated ethenes (*11*−*15*). Factors of importance for use of this organism in bioremediation systems include (a) competitive inhibition of contaminant conversion by the growth substrate; (b) toxicity of the cometabolic conversion products leading to both sMMO inactivation and cell death (*6*, *15*, *16*); and (c) regeneration of reducing equivalents (NADH) that are utilized in the cometabolic conversion of the contaminants.

In the preceding article (*1*), a biochemical model was presented that describes growth of *M. trichosporium* OB3b. The model explicitly includes the cofactor NADH, the regeneration of which is incorporated by taking into account catabolism, biosynthesis, and poly-β-hydroxybutyric acid (PHB) metabolism. In this paper, this model

* Tel: (31)-(0)50-3634333. Fax: (31)-(0)50-3634479. E-mail: K.J.Ganzeveld@chem.rug.nl.
[†] Chemical Engineering Department.
[‡] Biochemistry Department.

10.1021/bp990155e CCC: $19.00
Published on Web 03/02/2000

is extended to incorporate the cometabolic conversion of the contaminants.

Although several models have been proposed to describe cometabolism (*17*−*21*), only Chang and Alvarez-Cohen (*22*) explicitly consider NAD(P)H limitation. Their model assumes reducing equivalent regeneration to result from endogenous and added external substrates, but the metabolic pathways linking these compounds are not incorporated. Evaluation of alternative strategies to enhance TCE conversion, such as the use of methanol or formaldehyde, is therefore not possible. Incorporation of a more detailed description can also improve the understanding of the metabolic processes involved in NADH regeneration, as illustrated by the use of PHB as a sink for reducing equivalents (*1*).

This contribution presents a model that integrates growth of strain OB3b with contaminant (TCE) conversion. Besides a description of NADH regeneration, the model incorporates the TCE conversion kinetics, the competitive inhibition between TCE and methane, and the enzyme inactivation and cell death caused by the toxicity of the cometabolic conversion products. With parameters obtained from independent batch experiments, the model is applied to optimize TCE conversion in bioreactor systems. Model simulations and experimental data for the transformation of TCE using three different process configurations are discussed: (1) TCE transformation by a growing culture during continuous loading of TCE; (2) TCE transformation by a growing culture during pulsed loading of TCE; and (3) TCE transformation by a nongrowing culture during continuous loading of TCE using small amounts of methane to provide reducing equivalents.

Material and Methods

M. trichosporium OB3b was grown under copper limitation in a 3-L chemostat with methane as the sole carbon source as described by Sipkema et al. (*23*). TCE pulse experiments were performed by injecting pure TCE using a heat-sterilized glass syringe (5−100 mL). To ensure that TCE dissolved rapidly, it was injected with a long needle (20 cm) in the most turbulent zone of the bioreactor. Steady-state determination (biomass, NADH, PHB, dissolved oxygen, and inlet and outlet O_2 and CH_4 concentrations) and analytical techniques (biomass, NADH, PHB, O_2, CH_4, TCE) were performed as described by Sipkema et al. (*1*, *23*, *24*). Procedures used to determine the rate of TCE transformation in batch experiments were described by van Hylckama Vlieg et al. (*15*, *16*).

The two-step system used consists of a 3-L chemostat (growth reactor) as described above, coupled to a thermostated 17-L column reactor (conversion reactor). Flows of tap water, dissolved TCE, and cells (without gas) were combined (rate 110 mL min^{-1}) and fed to the conversion reactor. Via seven evenly distributed Teflon tubes (diameter 0.1 mm), fitted into the bottom plate, gas (air, CH_4) was supplied to the conversion reactor at a very low flow rate (45 mL min^{-1}, superficial velocity 0.04 mm s^{-1}) to minimize stripping of the contaminants. TCE conversion was calculated from the TCE concentrations measured in the inlet (liquid) and outlet (liquid, gas) of the conversion reactor. Further details are given in Sipkema et al. (*24*).

In all experiments described, a temperature of 30 °C was maintained. Mass transfer coefficients (k_La) for oxygen and methane in the chemostat system were derived as described in Sipkema et al. (*23*). The k_La for TCE in the chemostat and the k_La for methane and TCE used in the two-step system were derived from the k_La for oxygen using the square root of the ratio of the diffusion coefficients (*25*) (O_2, 2.6×10^{-9} m^2 s^{-1}; TCE, 1.17×10^{-9} m^2 s^{-1}; CH_4, 1.49×10^{-9} m^2 s^{-1}). Model calculations were performed as described in Sipkema et al. (*24*).

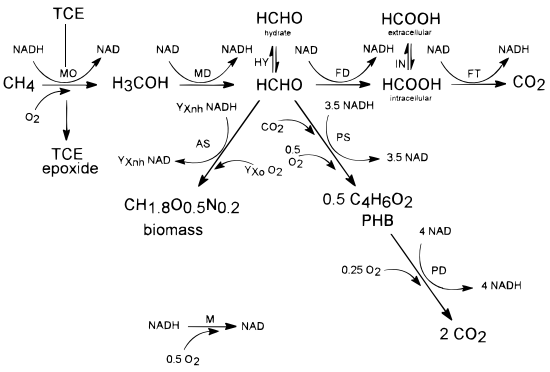

Figure 1. Schematic representation of growth of *M. trichosporium* OB3b and TCE conversion as incorporated in the model. ATP and acetyl-CoA were eliminated as described in the preceding article. Stoichiometry of each of the conversion steps is included, with NADH = $NADH_2$, $Y_{Xo} = 0.25\alpha - 0.55$, and $Y_{Xnh} = 0.5\alpha - 0.2$ ($\delta = 2$). H_2O and HNO_3 are not shown.

Model Development

The model describes the concomitant processes of growth of *M. trichosporium* OB3b and cometabolic TCE conversion and calculates biomass, storage material (PHB), TCE, and substrate concentrations as a function of time. Details of the growth part of the model (structure, system definition, stoichiometry, and kinetics) were described in the preceding article and are summarized here briefly. The TCE part of the model is discussed in detail.

Growth of *M. trichosporium* OB3b. *M. trichosporium* OB3b converts methane via methanol to formaldehyde, which is either assimilated via the serine pathway into biomass or PHB or dissimilated via formate to carbon dioxide (Figure 1). All of these compounds, as well as NADH, biomass, and oxygen, are included in the model as dynamic pools, their concentrations changing with time. ATP is assumed to be in equilibrium with NADH via oxidative phosphorylation. Stoichiometry (see Figure 1) is based on the metabolic pathways. All enzymatic reactions are described by Michaelis−Menten type equations, with a separate term for each limiting (co)-substrate. For formate, transport across the membrane is considered, which is described as a fully reversible enzymatic reaction. For formaldehyde, which in diluted aquatic solutions is present mostly in its hydrated form, a first-order dehydration reaction is included. The strong dependence of PHB formation on NADH is described by a Hill equation. The PHB degradation rate reaction (q_{PD} [mol s^{-1} kg^{-1}], Table 1) includes a NADH-dependent inhibition term that ensures negligible PHB turnover under steady-state conditions while enabling PHB mobilization at very low NADH levels. Finally, under growth conditions (specific growth rate $\mu > 25\%$ μ_{MAX}), maintenance is neglected, while under conditions of prolonged absence of the growth substrate, it is included with a rate q_M (Table 1), leading to NADH and oxygen consumption. A complete overview of the kinetic equations incorporated in the growth part of the model is given in the preceding article.

Table 1. Kinetic Equations and Parameter Values Describing Maintenance and PHB Degradation in the Growth Model of *M. trichosporium* OB3b

Kinetic Equations

$$q_M = M\left(\frac{C_{nh}}{C_{nh}+K_{M,M,nh}}\right)\left(\frac{C_{L,o}}{C_{L,o}+K_{M,M,o}}\right)$$

$$q_{PD} = V_{MAX,PD}\left(\frac{C_b}{C_b+K_{M,PD,b}}\right)\left(\frac{C_n}{C_n+K_{M,PD,n}}\right)\left(\frac{C_{L,o}}{C_{L,o}+K_{M,PD,o}}\right)\left(\frac{1}{1+C_{nh}/K_{I,PD,nh}}\right)$$

with

$$K_{I,PD,nh} = K_{I,PD,MAX}\left(1-\frac{C_{nh}^{w}}{C_{nh}^{w}+K_{M,PD,SP}^{w}}\right)+K_{I,PD,MIN}\left(\frac{C_{nh}^{w}}{C_{nh}^{w}+K_{M,PD,SP}^{w}}\right)$$

Parameter Values

enzyme system	parameter	value	unit
M	M	6.4×10^{-5}	mol s^{-1} kg^{-1}
	$K_{M,M,nh}$	1.0×10^{-4}	mM
	$K_{M,M,o}$	1.0×10^{-4}	mM
PD	$V_{MAX,PD}$	1.4×10^{-4}	mol s^{-1} kg^{-1}
	$K_{M,PD,b}$	1.0	mM
	$K_{M,PD,SP}$	0.015	mM
	$K_{I,PD,MAX}$	4.1×10^{-4}	mM
	$K_{I,PD,MIN}$	1.0×10^{-8}	mM
	w	10	

TCE-Related Processes. Cometabolic TCE conversion by strain OB3b results in two individually identifiable and measurable effects (*16*): (1) loss of enzyme (sMMO) activity, quantified by the transformation capacity T_C [mol kg^{-1}] and (2) loss of viability, quantified by LAT_{50} [mol kg^{-1}], the amount of TCE transformed per unit of cell mass resulting in a 50% decrease in the number of viable cells.

The first effect is taken into account by incorporating in the model the fraction of active enzyme (sMMO) E and the second effect by distinguishing between dividing cells (concentration C_{Xdiv} [kg L^{-1}]) and nondividing cells (C_{Xnon}). Only the dividing cells grow and as a result of TCE transformation loose their dividing capacity and become nondividing cells. This is described by I_{CD} [kg mol^{-1}], the cell death related inactivation constant, that is linked to LAT_{50} via $I_{CD} = \ln(2)/LAT_{50}$. The factor ln(2) follows from the translation of LAT_{50}, which represents a process of chance acting on the whole population, to I_{CD}, which represents a linear process acting on the viable population only.

As a result of the growth of new cells and of the loss of dividing capacity of existing (dividing) cells, the amount of active sMMO of dividing cells differs from the amount of active sMMO of nondividing cells (see below). Therefore, a distinction is made between E_{div}, the active fraction sMMO of the dividing cells, and E_{non}, the active fraction sMMO of the nondividing cells. When part of the cells have lost their dividing capacity as a result of TCE transformation, decoupling occurs; the methane converted by the active sMMO of the nondividing cells does not lead to cell growth and the observed growth yield on methane decreases. Thus all of the active sMMO, both in dividing and in nondividing cells, is assumed to convert methane and TCE. To incorporate this, the active enzyme (sMMO) fraction ϵ is introduced:

$$\epsilon = \frac{E_{div}\,C_{Xdiv} + E_{non}\,C_{Xnon}}{C_{Xtot}} \tag{1}$$

with C_{Xtot} the total cell concentration ($= C_{Xdiv} + C_{Xnon}$). The specific methane conversion rate $q_{MO,m}$ [mol s^{-1} kg^{-1}], discussed in the preceding article, then becomes

$$q_{MO,m} = \epsilon V_{MAX,MO,m}\left(\frac{C_{L,m}}{C_{L,m}+K_{M,MO,m,app}}\right)\times \left(\frac{C_{nh}}{C_{nh}+K_{M,MO,nh}}\right)\left(\frac{C_{L,o}}{C_{L,o}+K_{M,MO,o}}\right) \tag{2}$$

with the subscripts m = methane, nh = NADH, and o = oxygen, where $V_{MAX,MO,j}$ is the maximum specific conversion rate of compound j by sMMO [mol s^{-1} kg^{-1}], $K_{M,MO,j}$ is the affinity constant of sMMO for compound j [mol L^{-1}], $C_{L,j}$ is the overall and C_j the intracellular compound concentration [mol L^{-1}]. $K_{M,MO,m,app}$, the apparent affinity constant of sMMO for methane [mol L^{-1}], is introduced to incorporate the effect of competitive inhibition between methane and TCE:

$$K_{M,MO,m,app} = K_{M,MO,m}\left(1+\frac{C_{L,t}}{K_{M,MO,t}}\right) \tag{3}$$

where the subscript t = TCE. Because TCE as well as methane are converted by sMMO, similar expressions are used for the specific conversion rate of TCE ($q_{MO,t}$ [mol s^{-1} kg^{-1}]):

$$q_{MO,t} = \epsilon V_{MAX,MO,t}\left(\frac{C_{L,t}}{C_{L,t}+K_{M,MO,t,app}}\right)\times \left(\frac{C_{nh}}{C_{nh}+K_{M,MO,nh}}\right)\left(\frac{C_{L,o}}{C_{L,o}+K_{M,MO,o}}\right) \tag{4}$$

and for the apparent affinity constant of sMMO for TCE, $K_{M,MO,t,app}$:

$$K_{M,MO,t,app} = K_{M,MO,t}\left(1+\frac{C_{L,m}}{K_{M,MO,m}}\right) \tag{5}$$

Only dividing cells with active sMMO grow, and therefore the fraction of the total amount of active sMMO that is present in dividing cells, β, is introduced:

$$\beta = \frac{E_{div}C_{Xdiv}}{E_{div}C_{Xdiv}+E_{non}C_{Xnon}} \tag{6}$$

Hence, the specific growth rate μ [s^{-1}] is

$$\mu = \beta Y_{Xfd} q_{AS} \tag{7}$$

with q_{AS} the flux through the assimilation pathway and Y_{Xfd} the yield of biomass on formaldehyde [kg mol^{-1}]. The increase in total cell population becomes

$$\frac{dC_{Xtot}}{dt} = \mu C_{Xdiv} \tag{8}$$

The dividing cell population increases as a result of growth, but decreases as a result of cell death caused by TCE transformation as described by I_{CD}:

$$\frac{dC_{Xdiv}}{dt} = \mu C_{Xdiv} - I_{CD} q_{MO,t} C_{Xdiv} \tag{9}$$

Finally, the nondividing cell population, C_{Xnon}, follows from the cell balance ($C_{Xtot} = C_{Xdiv} + C_{Xnon}$).

Changes in E_{div} and E_{non} occur as a result of the TCE transformation described by T_C and as result of the changes in the cell populations (eqs 8 and 9). When new

Table 2. Values for Parameters Related to Methane and TCE Conversion in the Model for *M. trichosporium* OB3b.

parameter	value	unit	source
		Kinetics	
$V_{MAX,MO,m}$	6.1×10^{-3}	mol s^{-1} kg^{-1}	Oldenhuis et al. (*6*)
$K_{M,MO,m}$	0.037	mM	Sipkema et al. (*23*)
$V_{MAX,MO,t}$	0.011	mol s^{-1} kg^{-1}	this work, batch experiments
$K_{M,MO,t}$	0.145	mM	Oldenhuis et al. (*6*)
$K_{M,MO,nh}$	0.050	mM	Fox et al. (*26*)
$K_{M,MO,o}$	0.013	mM	Green and Dalton (*27*)
		Toxicity of TCE Conversion Products	
I_{CD}	2.3	kg mol^{-1}	Van Hylckama Vlieg et al. (*16*)
T_C	4	mol kg^{-1}	Van Hylckama Vlieg et al. (*16*)

dividing cells are formed, E_{div} increases proportional to $(1 - E_{div})$, the difference between the sMMO activity of the new cells and that of the current population:

$$\frac{dE_{div}}{dt} = -\frac{1}{T_C} q_{MO,t} + (1 - E_{div})\,\mu\,\frac{C_{Xdiv}}{C_{Xtot}} \qquad (10)$$

Last, when cells lose their dividing capacity as a result of the TCE transformation described by I_{CD}, E_{non} changes proportional to $(E_{div} - E_{non})$:

$$\frac{dE_{non}}{dt} = -\frac{1}{T_C} q_{MO,t} + (E_{div} - E_{non})\, I_{CD}\, q_{MO,t}\,\frac{C_{Xdiv}}{C_{Xtot}} \qquad (11)$$

Substrate concentrations as a function of time are obtained by simultaneously solving the set of differential equations that consists of mass balances incorporating stoichiometry and enzyme kinetics as discussed above, as well as reactor-specific mass transfer expressions (*23*). Balances were included for enzyme activity (E_{div}, E_{non}), biomass (C_{Xdiv}, C_{Xnon}, C_{Xtot}), and the compounds methane, methanol, formaldehyde, formate, NAD(H), PHB, oxygen, and TCE.

Parameter Estimation. Parameters of the growth part of the model were either taken from literature, measured in independent batch experiments, or estimated from steady-state chemostat data (α, δ) or dynamic chemostat data (V_{MAX}, K_M) as discussed in the preceding article. Parameters related to maintenance and PHB degradation were derived from batch experiments performed under starvation conditions and from experimental data obtained under NADH-limiting conditions in a two-step system (see Results) (Table 1). The complete set of growth-related parameters is given in the preceding article.

Parameters related to methane and TCE conversion ($K_{M,MO,j}$, $V_{MAX,MO,j}$, I_{CD}, T_C) were either taken from literature or determined in batch experiments using cells harvested from a continuous culture of strain OB3b (Table 2). Because of the low solubility of TCE in the medium and the overall mass transfer rate in the batch reactor, only low TCE concentrations (0−0.03 mM) were used in the experiments. These concentrations were always far below the OB3b affinity constant of sMMO for TCE ($K_{M,MO,t} = 0.145$ mM, Table 2). Therefore a TCE conversion rate constant first order in TCE ($k_t = V_{MAX,MO,t}/K_{M,MO,t}$) was determined. From this TCE rate constant, the V_{MAX} of sMMO for TCE incorporated in the model ($V_{MAX,MO,t}$) was calculated using $K_{M,MO,t} = 0.145$ mM (*6*). The value of the V_{MAX} for TCE ($V_{MAX,MO,t}$, Table 2) was based on seven independent batch experiments. Although these batch experiments were performed with cells with a very different culture history (dilution rates ranging from 30% to 90% of the maximum growth rate), the kinetic data obtained was very similar, within an experimental error of 10%. Therefore the value of V_{MAX} presented in Table 2 is an average of these results.

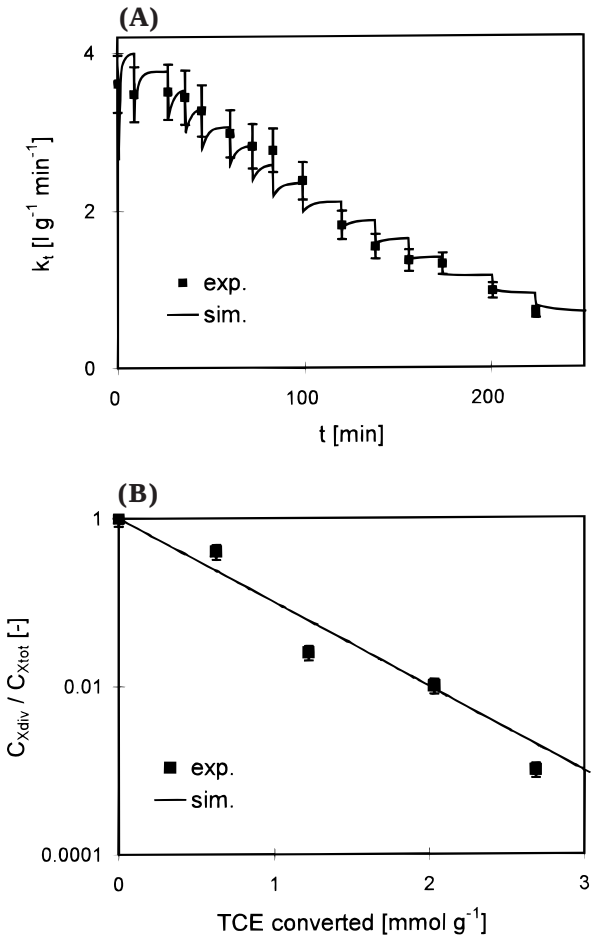

Figure 2. Conversion of repeated injections of TCE in a batch experiment using cells of strain OB3b freshly harvested from a continuous culture growing on methane. (A) Experimental results and model prediction (with $k_t = q_{MO,t}/C_{L,t}$) of the effect on sMMO activity as a function of time. (B) Experimental data from van Hylckama Vlieg et al. (*16*) and model prediction of the effect on cell viability as a function of the cumulative amount of TCE converted. Chemostat: $C_{Xtot} = 0.6$ g L^{-1}; $D = 0.024$ h^{-1}; $\epsilon = 1$. Formate concentration batch experiments = 20 mM.

Results and Discussion

The negative effects of TCE conversion on the cells (enzyme inactivation, loss of viability) were quantified by van Hylckama Vlieg et al. (*16*) in batch experiments using cells freshly harvested from a continuous culture. These experimental data and experimental data obtained in similar batch experiments are compared with model predictions and used to illustrate the negative effects of TCE conversion. Subsequently, the model is validated and applied to optimize TCE conversion.

Effects of TCE Conversion on Resting Cells. In batch experiments with sufficient NADH available (20 mM formate), the negative effect of TCE conversion on enzyme (sMMO) activity was visible as a decrease in the rate constant for TCE conversion (k_t) (Figure 2A). The model, in which this was incorporated via the active enzyme fraction ϵ, gave a rather accurate description of the experimental data (Figure 2A) using TCE related

parameter values from literature (T_C, I_{CD}, $K_{M,MO,t}$) and a TCE V_{MAX} value from independent batch experiments (k_t, see Table 2).

In the same type of batch experiments, Van Hylckama Vlieg et al. (*16*) observed a negative effect of TCE conversion on the viability of the culture (Figure 2B). The model appears to describe these data accurately by incorporating the cell death constant I_{CD} and distinguishing dividing from nondividing cells (Figure 2B).

To compare the different types of toxic effects of the TCE conversion products on the cells, the ratio between the amount of substrate converted per unit of cell mass that caused a 50% decrease in enzyme activity (0.5 T_C) and the LAT_{50} was calculated. The ratio (0.5 T_C/LAT_{50}) appeared to be 6.6 (Table 2), which indicates that TCE conversion affected viability more strongly than enzyme activity. This appears to be true for most chlorinated ethenes except for chloroethene (*16*).

Optimization of TCE Conversion. In the preceding article, it was shown that the model gave a good accurate description of the experimental data collected for growth of strain OB3b under various conditions (*1*). The model now also appears to describe TCE conversion measured for a resting cell culture realistically. Of course, there are still some discrepancies between experimental data and the model. However, the results are remarkably good, and trends and values are predicted within the experimental error. Thus, TCE conversion appears to be correctly incorporated in the model, implying that the model can be used to evaluate strategies of practical interest. Situations considered are aimed at process optimization and include (I) a growing culture subjected to a continuous load of TCE; (II) a growing culture subjected to a pulsed load of TCE; and (III) a nongrowing culture subjected to a continuous load of TCE.

By comparing simulations with experimental results, the situations discussed below also serve as an extra validation of the model. This extra validation is necessary because the situations considered previously (Figure 2) were similar or equal to those used for the determination of the parameters of TCE conversion (e.g. I_{CD}, T_C).

Case I. A Growing Culture Subjected to a Continuous Load of TCE. Since TCE conversion more strongly affects viability than enzyme activity (0.5 $T_C/LAT_{50} = 6.6$), in systems in which growth of the cells and TCE conversion are combined, yields are expected to decrease rapidly with increasing load of TCE. TCE conversions (ζ_{TCE}) on the other hand are expected to remain very high, up to the point where wash-out occurs.

Model calculations of a chemostat culture subjected to increasing TCE loads confirmed these expectations. They showed a 50% decrease in yield with increasing inlet TCE gas concentration, while TCE conversions remained as high as 95%, up to the point of wash-out (Figure 3). This same situation was measured by Oldenhuis (*28*), and his experimental results are close to model predictions (Figure 3). In addition, the point at which wash-out occurred was predicted correctly, although it had not been determined very exactly, at between 0.55 and 3.1 mM, where the model calculated 1.6 mM. Unfortunately this experimental determination of the exact point of wash-out is very difficult and much dependent on small changes in equipment performance. Therefore, an absolute confirmation of the prediction of the model cannot be obtained.

Case II. A Growing Culture Subjected to a Pulsed Load of TCE. In many practical situations, such as industrial wastewater treatment, TCE loads are pulsed rather than constant. This effect was simulated as a series of pulses of TCE injected in a continuous culture. On the basis of expectations concerning the rate of cell death (resulting from small amounts of TCE converted) and enzyme inactivation (resulting from large amounts), pulses of increasing size were used. With 1 h intervals, five fairly small pulses were first injected (injected TCE concentrations $C_{L,t,inj} = 0.014-0.048$ mM), followed by five larger ones ($C_{L,t,inj} = 0.33-0.64$ mM).

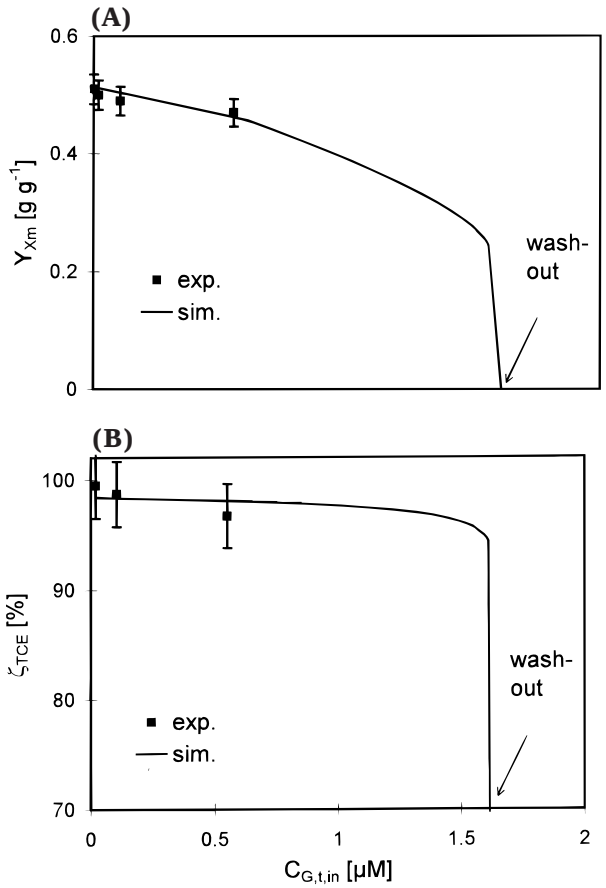

Figure 3. Effect of increasing inlet TCE gas concentration on a continuous culture of strain OB3b growing on methane. Model simulation and experimental results of Oldenhuis (*28*) for (A) yield on methane and (B) TCE conversion, as a function of the inlet TCE gas concentration. $C_{Xtot}(C_{G,t,in} = 0) = 2.5$ g L^{-1}; $D = 0.028$ h^{-1}; $V_L = 650$ mL; $C_{G,m,in} = 6.6$ mM; $C_{G,o,in} = 9.4$ mM; $k_La_m = 1.2$ min^{-1}; $k_La_o = 1.7$ min^{-1}; $\phi_G = 44$ mL min^{-1}.

With each pulse, a decrease in cell viability (C_{Xdiv}) was calculated, leaving the culture effectively "dead" after injection of the first large pulse (0.33 mM) (Figure 4A).

sMMO activity, on the other hand, appeared to be hardly affected by the small pulses ($C_{L,t,inj} < 0.33$ mM) and only decreased after injection of the large pulses ($C_{L,t,inj} = 0.33-0.64$ mM) (Figure 4B). Even though the culture is calculated to be largely nonviable after the first 0.33 mM pulse, effective conversion of considerable amounts of TCE still occurs (Figure 4C). In fact, conversions are calculated to remain above 99.8% with each additional pulse, up to the last one, which is still converted for 87%.

The simulation was verified by an experiment carried out with a 3-L culture grown at $D = 0.028$ h^{-1}. The results were found to confirm the accuracy of the model predictions (Figures 4A and 4B). The model therefore gives a good description of these types of pulsed experiments.

Case III. A Nongrowing Culture Subjected to a Continuous Load of TCE. As illustrated by the pulse

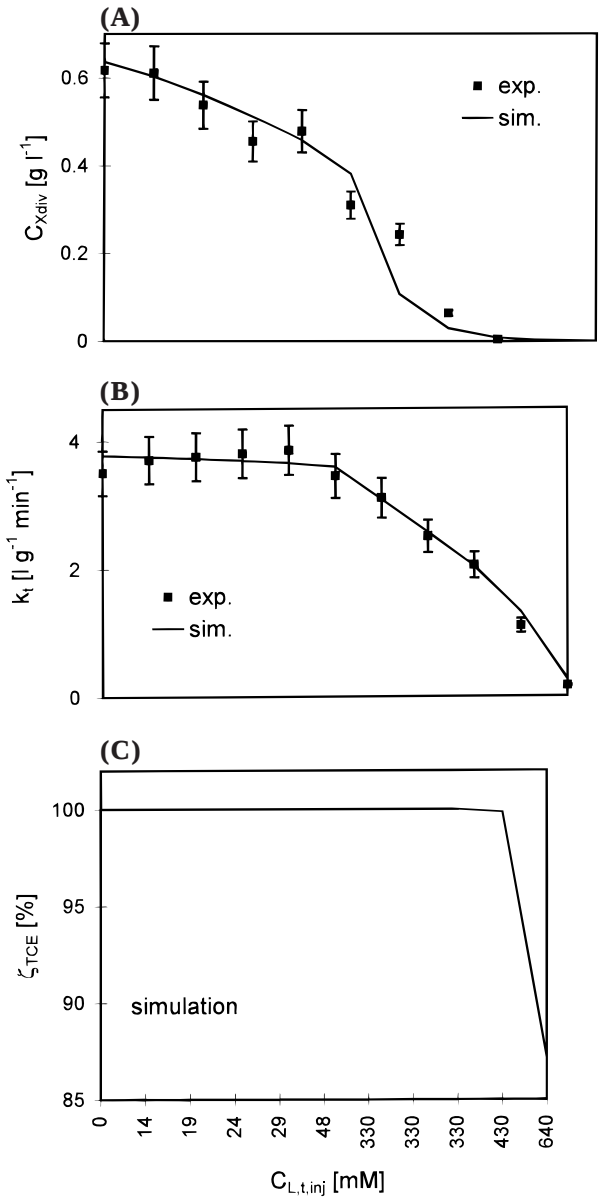

Figure 4. Effect of sequentially injected TCE pulses of increasing size on a continuous culture of strain OB3b growing on methane. Model simulation and experimental results showing the effect on (A) cell viability, (B) sMMO activity, and (C) TCE conversion (mind the *y*-axis scale), as a function of injection number identified by injected TCE concentration ($C_{L,t,inj}$). Prior to the experiment $C_{Xtot} = 0.64$ g L^{-1} and $\epsilon = 1$; $D = 0.028$ h^{-1}.

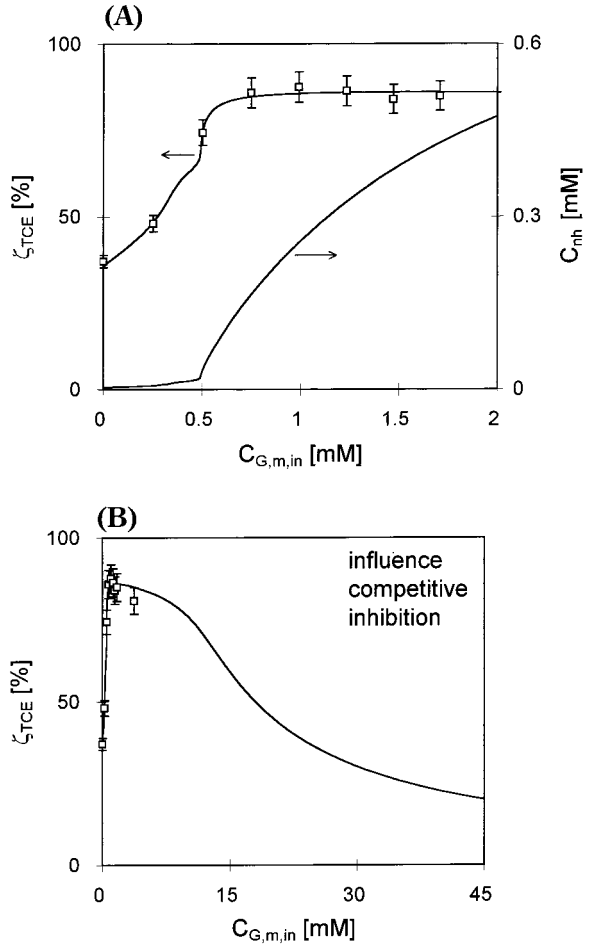

Figure 5. Effect of increasing methane concentration in the conversion reactor of the two-step system on TCE conversion by strain OB3b. (A) Small amounts of methane in the inlet, no competitive inhibition visible. The NADH levels calculated with the model are also included (right axis). (B) Large amounts of methane in the inlet, competitive inhibition visible. $C_{L,t,in} = 0.019$ mM; $C_{Xtot,in} = 19$ mg L^{-1}; $\epsilon_{in} = 1$; $C_{b,in} = 1$ wt %; $\tau = 2.6$ h; $V_L = 17$ L; $\phi_G = 45$ mL min^{-1}. □, experimental data; (−)=model.

experiment discussed above, a culture that is no longer viable can still convert a large amount of TCE. Therefore, growth-based systems, the design of which is based on the necessity to compensate for cell death rather than for enzyme inactivation only, generally do not make efficient use of the conversion capacity of the cells. This also holds for biofilm systems, in which clogging of the system with dead and inactive biomass, which occurs with time, will deteriorate performance. A better strategy is to use a two-step system, in which growth of the cells is separated from TCE conversion. Similar conclusions have been drawn previously by others (*6*, *17*, *29*−*32*), but primarily based on competitive inhibition considerations.

In two-step systems, the full conversion capacity of the cells (T_C) can be used, after which the nonviable cells are discarded. Energy (NADH) limitation, occurring in the second step of the system, can be alleviated by adding sufficient formate or small amounts of methane. The problem of stripping of the contaminants, associated with the use of a gas phase to add methane, can be overcome by using very small gas flows, as illustrated in the system described by Sipkema et al. (*24*).

Model predictions of a two-step system with methane addition in the second step show that, as a result of low NADH levels, TCE conversion rates are low under the starvation conditions in the second step ($C_{G,m,in} \approx 0$, Figure 5A). When sufficient methane is added ($C_{G,m,in} \approx 0.55$ mM), NADH levels increase, which leads to a rapid increase in TCE conversion (Figure 5A). Furthermore, calculations for larger methane additions show that competitive inhibition between TCE and methane does not become a problem until far more than the optimal amount of methane is added (Figure 5B).

An experimental setup with a volume of 17 L, which was built to test this application and which is addressed in detail elsewhere (*24*), confirmed the observations (Figure 5A).

In batch experiments performed with cells freshly harvested from a continuous culture, measurements of the initial TCE conversion rate under NADH-limiting conditions (no electron donor added) appeared to be poorly reproducible, with k_t values ranging from 1.4 to 2.7 L g^{-1} min^{-1}. Thus, characterization of the cells under

these conditions in the two-step system ($C_{G,m,in} < 0.6$ mM, Figure 5A), necessary to simulate TCE conversion, is difficult. Therefore, the parameters describing this situation (initial conditions, maintenance requirements, PHB mobilization) were estimated from batch experimental data as well as from the two-step experimental data (Figure 5A) (parameter values, Table 1). It follows that the model's predictive capacity is limited in this region. However, independent of the precise value of the parameters, the model does predict a transition from low to high TCE conversion at increasing influent methane concentration, as is observed experimentally (Figure 5A). For practical purposes therefore, based on batch experiments, a rough estimate of the actual transition point (in the setup of Figure 5A, $C_{G,m,in} = 0.5-0.6$ mM) and thus of the minimum amount of methane needed for optimal TCE conversion (Figure 5A, $C_{G,m,in} > 0.6$ mM) can be calculated. Since the optimum in the TCE conversion is broad (Figure 5B), an overestimation of the amount of methane needed, e.g., by a factor of 2, will subsequently ensure optimal TCE conversions without risking a deterioration of system performance due to competitive inhibition.

TCE conversion under NADH-limiting conditions ($C_{G,m,in} < 0.6$ mM, Figure 5A) is determined both by the amount of NADH initially available and by the amount of NADH produced as a result of PHB mobilization. Therefore, it is expected that cells with a higher PHB content will convert more TCE. Although we did not test this ourselves, batch experiments performed by Shah et al. (*33*), in which cells of strain OB3b were grown under nitrogen limitation, verify this conclusion. They found that higher PHB levels correlated with higher T_C values, implying a higher TCE conversion in a two-step system. At a PHB content of 10 wt %, they found that the T_C values no longer increased with increasing PHB content. Because at this point T_C values were still 40% lower than with excess electron donor (formate) present, the positive effect of PHB mobilization as a means to regenerate NADH appears to be limited. Furthermore, nitrogen-limiting conditions can cause culture instabilities, suggesting that growth of strain OB3b under carbon limitation with small amounts of methane added in the TCE conversion reactor as exogenous electron donor may be a more secure, as well as a more feasible, strategy to obtain optimal TCE conversions.

Optimization of TCE Conversion. Comparison of Growing and Nongrowing Systems. To enable a direct comparison of the TCE conversion obtained in a growing system and in a nongrowing system, model calculations were performed for a bioreactor that was subjected to an increasing liquid load of TCE. In the first case, growth of the cells and TCE conversion were combined. In this single-step system or chemostat, either methane or methane and methanol were used as growth substrates. In the second case, the cells were grown in one bioreactor (A) and added to a second bioreactor (B) via the inlet. Bioreactor B, which can be considered as the second step in a two-step system, was subjected to increasing TCE flow, while small amounts of methane were added as electron donor. The cells added to B via the inlet were grown in A under conditions identical to those of the first case, without TCE present. Both the bioreactor of the single-step and that of the two-step system had identical volumes and gas and liquid flows.

As observed above, with an increase of the load of TCE in the single-step system wash-out occurs very rapidly, and only small amounts of TCE can be converted (Figure 6). When 25% of the methane (0.25 $C_{G,m,in}$) is substituted

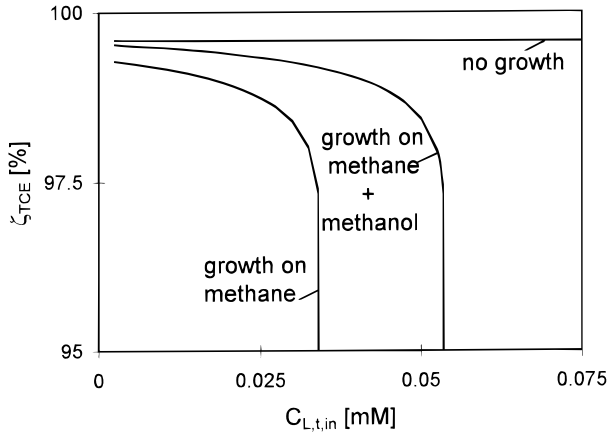

Figure 6. Model calculation showing the difference between TCE conversion in a growing system of strain OB3b and in a nongrowing (two-step) system without electron-donor addition. TCE conversion as a function of the inlet TCE liquid concentration, for (1) growth on methane ($C_{G,m,in} = 9.3$ mM; $C_{Xtot}(C_{L,t,in} = 0) = 0.52$ g L^{-1}; $\epsilon(C_{L,t,in} = 0) = 1$; $D = 0.048$ h^{-1}); (2) growth on methane ($C_{G,m,in} = 7$ mM) and methanol ($C_{L,ml,in} = 20$ mM) (C_{Xtot}-$(C_{L,t,in} = 0) = 0.52$ g L^{-1}; $\epsilon(C_{L,t,in} = 0) = 1$; $D = 0.048$ h^{-1}); and (3) two-step system without electron-donor addition ($C_{Xtot,in} = 0.52$ g L^{-1}; $\epsilon_{in} = 1$; $C_{G,m,in} = 0$; $\tau = 21$ h). $V_L = 2.5$ L; $\phi_G = 41$ mL min^{-1}.

by an amount of methanol sufficient to maintain the original cell density ($C_{L,ml,in} = 20$ mM), less competitive inhibition appears to occur, and conversions slightly increase (Figure 6). Since conversion of methane to methanol costs energy (NADH) (Figure 1), a higher biomass concentration is obtained, and 60% more TCE can be converted before wash-out (Figure 6). In both cases, though, TCE conversion appears to be limited by cell death, and enzyme activity is hardly utilized ($\zeta_{TCE} >$ 95%). This is demonstrated by the nongrowing system, where cell death does not play a role and very high conversions (no competitive inhibition) can be maintained (Figure 6).

At far higher TCE loads (>10-fold), TCE conversion in the two-step system decreases as a result of NADH limitation and loss of enzyme activity. Without NADH donor (methane) addition, NADH limitation ($C_{nh} < 0.015$ mM) occurs around a TCE inlet concentration of ≈0.4 mM (Figure 7A), which leads to a rapid deterioration of the TCE conversion with a further increase in TCE inlet concentration (Figure 7B). At the start of NADH limitation ($C_{L,t,in} = 0.4$ mM), only ≈20% of the enzyme activity has been used (Figure 7C).

Adding small amounts of methane ($C_{G,m,in} = 0.1$ mM, increase $C_{Xtot} \approx 1\%$) to provide reducing equivalents postpones NADH limitation (Figure 7A) and leads to continuation of the high TCE conversions until a TCE inlet concentration of ≈1.3 mM (Figure 7B) and a utilization of a maximum of ≈70% of the enzyme activity (Figure 7C). A further increase in the TCE inlet concentration again results in NADH limitation ($C_{nh} < 0.015$ mM, Figure 7A). The NADH limitation blocks not only the TCE conversion but also the methane consumption, leading to a sudden drop in TCE conversion and a reversion to the situation without NADH donor addition (Figure 7B,C).

For still larger amounts of methane added (1 mM, increase $C_{Xtot} \approx 10\%$), enzyme activity is almost completely utilized ($\epsilon \rightarrow 0$, Figure 7C). Loss of enzyme activity causes a gradual decrease in TCE conversion (Figure 7B), up to the point where NADH finally becomes limited ($C_{L,t,in} \approx 3.4$ mM, Figure 7A). As with less methane

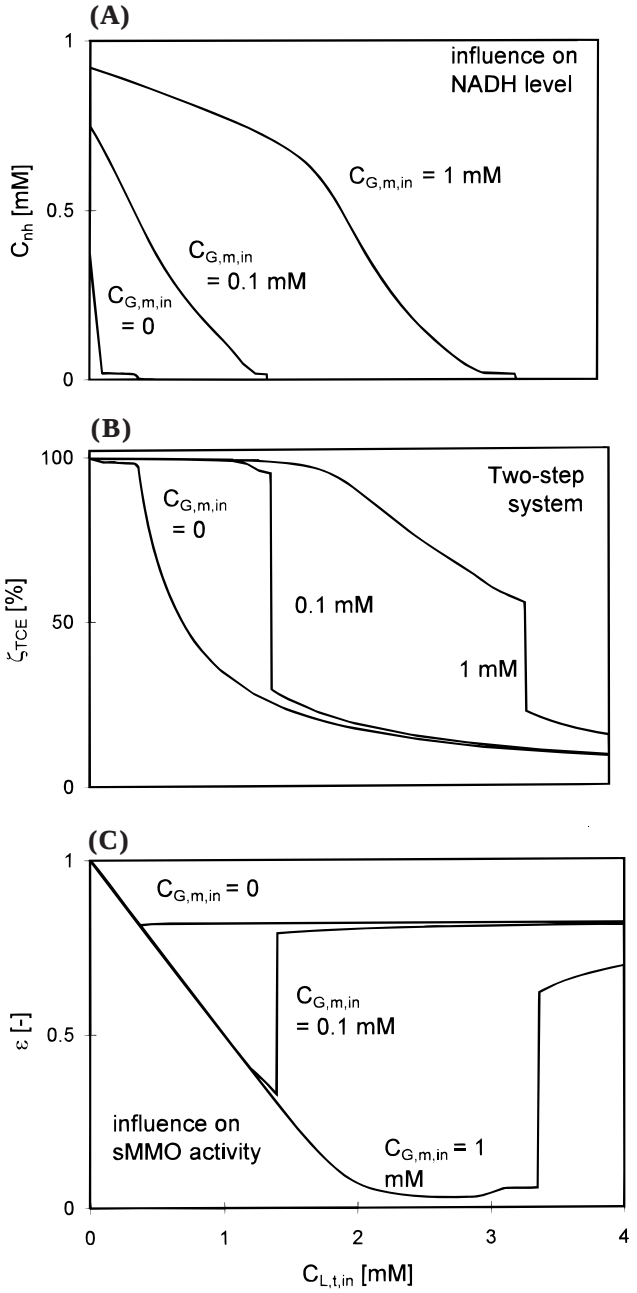

Figure 7. Model calculation showing the effect on TCE conversion by strain OB3b of NADH-donor addition to the conversion reactor of a two-step system. (A) NADH concentration, (B) TCE conversion, and (C) sMMO activity, as a function of the inlet TCE liquid concentration. Three situations are shown: (1) without methane addition (two-step system of Figure 6); (2) with $C_{G,m,in}$ = 0.1 mM (≈1% increase in C_{Xtot}); and (3) with $C_{G,m,in}$ = 1 mM (≈10% increase in C_{Xtot}). $C_{Xtot,in}$ = 0.52 g L^{-1}; ϵ_{in} = 1; $C_{b,in}$ = 1 wt %; τ = 21 h; V_L = 2.5 l; ϕ_G = 41 mL min^{-1}.

addition, NADH limitation causes a sudden decrease in TCE conversion ($C_{L,t,in}$ ≈ 3.4 mM, Figure 7B) and a sudden increase in remaining sMMO activity (Figure 7C). Therefore, depending on the TCE load, a minimal amount of NADH donor is needed for efficient use of enzyme activity.

On the basis of the simulations discussed (Figures 6-7), two-step systems with NADH donor addition in the second step appear to be most effective for practical application. Since methane is much cheaper than formate and generally very little is needed, it is preferable as NADH donor. Therefore, the model, which has proven reliable in describing situations of combined growth and TCE conversion such as occur in these types of two-step systems, provides a useful tool for design purposes.

Advantage Metabolic Model. The advantage of this more complicated model above simpler models lies in the possibility to evaluate strategies that involve the use of energy-supplying substrates with a complicated metabolic fate, such as methane or methanol. Also, reliable predictions concerning the use of other substrates, such as hydrogen (*34*), can reduce or even eliminate the need for extensive practical testing, after only a limited number of kinetic parameters has been determined.

Conclusions

A model is presented that describes the linked processes of growth of *M. trichosporium* OB3b and cometabolic TCE conversion. By explicitly incorporating the enzyme (sMMO) activity and distinguishing between dividing and nondividing cells, the model appears to accurately describe the experimentally determined effects of TCE conversion on enzyme activity and cell death. In suspended growth-based systems, with an increase in TCE load, wash-out occurs rapidly. Up to that point, enzyme activity is hardly affected, ensuring very high TCE conversions (>95%). Replacing methane by methanol does increase biomass concentrations, and therewith TCE conversions, but does not prevent wash-out at low TCE concentrations. Two-step systems, in which growth is separated from TCE conversion, appear to be more efficient. When sufficient methane is added as NADH donor in the second step, enzyme activity can be fully used, and an effective system for practical application is obtained.

The model realistically describes growth-based (single-step) systems subjected to a continuous and pulsed load of TCE, and a non-growth-based, two-step system subjected to a continuous load of TCE. It provides a useful tool for evaluating different bioremediation strategies, especially those in which substrates are used with a complicated metabolic fate.

Notation

Subscripts and Abbreviations

AS	assimilation (growth)
ATP	adenosine triphosphate
b	PHB
div	dividing cells
fd	formaldehyde
FD	formaldehyde dehydrogenase
ft	formate
FT	formate dehydrogenase
HY	dehydration reaction formaldehyde
IN	cellular membrane transport, directed intracellularly
in	in the ingoing flow
inj	injected (TCE pulses in continuous culture)
m	methane
M	maintenance
MD	methanol dehydrogenase
ml	methanol
MO	sMMO, soluble methane monooxygenase
n(h)	NAD(H)
NAD(H)	nicotinamide adenine dinucleotide (reduced/oxidized form)

non	nondividing cells
o	oxygen
PS	PHB synthesis
PD	PHB degradation
PHB	poly-β-hydroxybutyric acid
sMMO	soluble methane monooxygenase
t	TCE
TCE	trichloroethene
tot	total (= div + non)

Symbols

C_j	intracellular concentration of compound j [mol L^{-1}]
$C_{L,j}$	liquid concentration of compound j [mol L^{-1}]
$C_{G,j}$	gas-phase concentration of compound j [mol L^{-1}]
C_X	cell concentration [kg L^{-1}]
D	dilution rate (= f_L/V_L) [s^{-1}]
E	relative enzyme (sMMO) activity (fraction 0−1)
I_{CD}	(= ln(2)/LAT_{50}) inactivation constant related to cell death [kg mol^{-1}]
$K_{I,PD,nh}$	NADH-related inhibition constant for PHB degradation [mol L^{-1}]
$K_{I,PD,MAX}$	maximum $K_{I,PD,nh}$ leading to minimal inhibition by NADH [mol L^{-1}]
$K_{I,PD,MIN}$	minimum $K_{I,PD,nh}$ leading to maximal inhibition by NADH [mol L^{-1}]
$K_{I,PD,SP}$	set point below which PHB breakdown is enhanced [mol L^{-1}]
$k_L a$	volumetric mass transfer coefficient [s^{-1}]
$K_{M,i,j}$	affinity of enzyme system i for compound j [mol L^{-1}]
$K_{M,MO,j,app}$	apparent affinity constant of sMMO for compound j [mol L^{-1}]
k_t	= $V_{MAX,MO,t}/K_{M,MO,t}$, TCE conversion rate constant, first order in TCE [L s^{-1} kg^{-1}]
M	maximum rate of energy (mol NADH) consumption for maintenance [mol s^{-1} kg^{-1}]
LAT_{50}	amount of TCE transformed per unit of cell mass resulting in a 50% decrease in number of viable cells [mol kg^{-1}]
w	power in Hill term
$q_{i(j)}$	specific conversion rate (of compound j) by enzyme system i [mol s^{-1} kg^{-1}]
T_C	transformation capacity [mol kg^{-1}]
V_L	liquid volume [L]
$V_{MAX,i}$	maximum rate of enzyme system i [mol s^{-1} kg^{-1}]
Y_{Xfd}	growth yield of biomass on formaldehyde [kg mol^{-1}]
Y_{Xm}	growth yield of biomass on methane (j = nh, o, m) [kg kg^{-1}]
Y_{Xo}, Y_{Xnh}	C-mole of biomass formed per mol of oxygen or NADH consumed [mol mol^{-1}]

Greek Symbols

α	amount of energy (mol ATP) used per C-mole of biomass formed
β	fraction of total amount of active sMMO present in dividing cells
δ	(= P/O ratio), energy (mol ATP) produced per atom of oxygen used in oxidative phosphorylation
ϵ	active enzyme (sMMO) fraction
ζ_{TCE}	(overall) TCE conversion [%]
μ, μ_{MAX}	(maximum) specific growth rate [s^{-1}]
τ	residence time (= V_L/ϕ_L = 1/D) [s]
ϕ_G	gas flow rate [L s^{-1}]
ϕ_L	liquid flow rate [L s^{-1}]

References and Notes

(1) Sipkema, E. M.; De Koning, W.; Ganzeveld, K. J.; Janssen, D. B.; Beenackers, A. A. C. M. NADH-regulated metabolic model for growth of *M. trichosporium* OB3b. Model presentation, parameter estimation, and model validation. *Biotechnol. Prog.* **2000**, *16*, 176−188.

(2) Bouwer, E. J.; Zehnder, A. J. B. Bioremediation of organic compounds − putting microbial metabolism to work. *Trends Biotechnol.* **1993**, *11*, 360−367.

(3) MacDonald, J. A.; Kavanaugh, M. C. Restoring contaminated groundwater: an achievable goal? *Environ. Sci. Technol.* **1994**, *28*, 362−368.

(4) Love, T.; Eilers, R. G. Treatment of drinking water containing trichloroethylene and related industrial solvents. *J. Am. Water Works Assoc.* **1982**, *74*, 413−425.

(5) Hanson, R. S.; Hanson, T. E. Methanotrophic bacteria. *Microbiol. Rev.* **1996**, *60*, 439−471.

(6) Oldenhuis, R.; Oedzes, J. J.; Van der Waarde, J. J.; Janssen, D. B. Kinetics of chlorinated hydrocarbon degradation by *Methylosinus trichosporium* OB3b and toxicity of trichloroethylene. *Appl. Environ. Microbiol.* **1991**, *57*, 7−14.

(7) Burrows, K. J.; Cornish, A.; Scott, D.; Higgins, I. J. Substrate specificities of the soluble and particulate methane monooxygenase of *Methylosinus trichosporium* OB3b. *J. Gen. Microbiol.* **1984**, *130*, 3327−3333.

(8) Park, S.; Hanna, M. L.; Taylor, R. T.; Droege, M. W. Batch cultivation of *Methylosinus trichosporium* OB3b. I. Production of soluble methane monooxygenase. *Biotechnol. Bioeng.* **1991**, *38*, 423−433.

(9) Scott, D.; Brannan, J.; Higgins, I. J. The effect of growth conditions on intracytoplasmic membranes and methane monoxygenase activities in *Methylosinus trichosporium* OB3b. *J. Gen. Microbiol.* **1981**, *125*, 63−72.

(10) Stanley, S. H.; Prior, S. D.; Leak, D. J.; Dalton, H. Copper stress underlies the fundamental change in intracellular location of methane monooxygenase in methane-oxidizing organisms: studies in batch and continuous culture. *Biotechnol. Lett.* **1983**, *5*, 487−492.

(11) Little, C. D.; Palumbo, A. V.; Herbes, S. E.; Lidstrom, M. E.; Tyndall, R. L.; Gilmer, P. J. Trichloroethylene biodegradation by a methane-oxidizing bacterium. *Appl. Environ. Microbiol.* **1988**, *54*, 951−956.

(12) Oldenhuis, R.; Vink, R. L. J. M.; Janssen, D. B.; Witholt, B. Degradation of chlorinated aliphatic hydrocarbons by *Methylosinus trichosporium* OB3b expressing soluble methane monooxygenase. *Appl. Environ. Microbiol.* **1989**, *55*, 2819−2826.

(13) Tsien, H.; Hanson, R. S. Soluble methane monooxygenase component B gene probe for identification of methanotrophs that rapidly degrade trichloroethylene. *Appl. Environ. Microbiol.* **1992**, *58*, 953−960.

(14) Tsien, H.; Brusseau, G. A.; Hanson, R. S.; Wackett, L. P. Biodegradation of trichloroethylene by *Methylosinus trichosporium* OB3b. *Appl. Environ. Microbiol.* **1989**, *55*, 3155−3161.

(15) Van Hylckama Vlieg, J. E. T.; De Koning, W.; Janssen, D. B. Transformation kinetics of chlorinated ethenes by *Methylosinus trichosporium* OB3b and detection of unstable epoxides by on-line gas chromatography. *Appl. Environ. Microbiol.* **1996**, *62*, 3304−3312.

(16) Van Hylckama Vlieg, J. E. T.; De Koning, W.; Janssen, D. B. Effect of chlorinated ethene conversion on viability and activity of *Methylosinus trichosporium* OB3b. *Appl. Environ. Microbiol.* **1997**, *63*, 4961−4964.

(17) Alvarez-Cohen, L.; McCarty, P. L. A cometabolic biotransformation model for halogenated aliphatic compounds exhibiting product toxicity. *Environ. Sci. Technol.* **1991a**, *25*, 1381−1387.

(18) Alvarez-Cohen, L.; McCarty, P. L. Product toxicity and cometabolic competitive inhibition modeling of chloroform and trichloroethylene transformation by methanotrophic resting cells. *Appl. Environ. Microbiol.* **1991b**, *57*, 1031−1037.
(19) Broholm, K.; Christensen, T. H.; Jensen, B. K. Modelling TCE degradation by a mixed culture of methane-oxidizing bacteria. *Water Res.* **1992**, *26*, 1177−1185.
(20) Criddle, C. S. The kinetics of cometabolism. *Biotechnol. Bioeng.* **1993**, *41*, 1048−1056.
(21) Strand, S. E.; Bjelland, M. D.; Stensel, H. D. Kinetics of chlorinated hydrocarbon degradation by suspended cultures of methane-oxidizing bacteria. *Res. J. Water Pollut. Control Fed.* **1990**, *62*, 124−129.
(22) Chang, H. L.; Alvarez-Cohen, L. Model for the cometabolic biodegradation of chlorinated organics. *Environ. Sci. Technol.* **1995**, *29*, 2357−2367.
(23) Sipkema, E. M.; De Koning, W.; Ganzeveld, K. J.; Janssen, D. B.; Beenackers, A. A. C. M. Experimental pulse technique for the study of microbial kinetics in continuous culture. *J. Biotechnol.* **1998**, *64*, 159−176.
(24) Sipkema, E. M.; De Koning, W.; Ganzeveld, K. J.; Janssen, D. B.; Beenackers, A. A. C. M. Trichloroethene degradation in a two-step system by *M. trichosporium* OB3b. Optimization of system performance: use of formate and methane. *Biotechnol. Bioeng.* **1998**, *63*, 56−67.
(25) *Chemical Reactor Design and Operation*, 2nd ed.; Westerterp, K. R., van Swaaij, W. P. M., Beenackers, A. A. C. M., Eds.; J. Wiley and Sons Inc.: New York, 1984.
(26) Fox, B. G.; Froland, W. A.; Jollie, D. R.; Lipscomb, J. D. Methane monooxygenase from *Methylosinus trichosporium* OB3b. In *Hydrocarbons and Methylotrophy*; Lidstrom, M. E., Ed.; Methods in Enzymology; Academic Press Inc.: San Diego, 1990; Vol. 188, pp 191−202.
(27) Green, J.; Dalton, H. Protein B of soluble methane monooxygenase from *Methylococcus capsulatus* (Bath). *J. Biol. Chem.* **1985**, *260*, 15795−15801.
(28) Oldenhuis, R. Continuous degradation of trichloroethylene by *Methylosinus trichosporium* OB3b. In *Microbial degradation of chlorinated compounds. Application of specialized bacteria in the treatment of contaminated soil and wastewater*, Ph.D. Thesis; University of Groningen: Groningen, The Netherlands, 1992; pp 107−121.
(29) Chang, H. L.; Alvarez-Cohen, L. Two-stage methanotrophic bioreactor for the treatment of chlorinated organic wastewater. *Water Res.* **1997**, *31*, 2026−2036.
(30) Dobbins, D. C.; Peltola, J.; Kustritz, J. M.; Chresand, T. J.; Preston, J. C. Pilot-scale demonstration of a two-stage methanotrophic bioreactor for biodegradation of trichloroethylene in groundwater. *J. Air. Waste Manage. Assoc.* **1995**, *45*, 12−19.
(31) McFarland, M. J.; Vogel, C. M.; Spain, J. C. Methanotrophic cometabolism of trichloroethylene (TCE) in a two-stage bioreactor system. *Water Res.* **1992**, *26*, 259−265.
(32) Tschantz, M. F.; Bowman, J. P.; Donaldson, T. L.; Bienkowski, P. R.; Strong-Gunderson, J. M.; Palumbo, A. V.; Herbes, S. E.; Sayler, G. S. Methanotrophic TCE biodegradation in a multi-stage bioreactor. *Environ. Sci. Technol.* **1995**, *29*, 2073−2082.
(33) Shah, N. N.; Hanna, M. L.; Taylor, R. T. Batch cultivation of *Methylosinus trichosporium* OB3b: V. Characterization of poly-*beta*-hydroxybutyrate production under methane-denpendent growth conditions. *Biotechnol. Bioeng.* **1996**, *49*, 161−171.
(34) Shah, N. N.; Hanna, M. L.; Jackson, K. J.; Taylor, R. T. Batch cultivation of *Methylosinus trichosporium* OB3b: IV. Production of hydrogen-driven soluble or particulate MMO-activity. *Biotechnol. Bioeng.* **1995**, *45*, 229−238.

Accepted for publication January 7, 2000.

BP990155E